

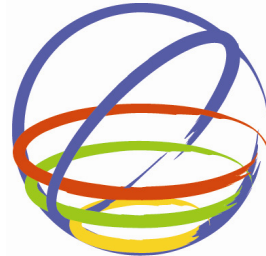
A New Ground Motion Prediction Equation Applicable Up To Mw9 Based on Data From the 2011 Tohoku-oki Earthquake

Nobuyuki Morikawa & Hiroyuki Fujiwara

National Research Institute for Earth Science and Disaster Prevention, Japan

Saburoh Midorikawa

Tokyo Institute of Technology, Japan



15 WCEE
LISBOA 2012

SUMMARY:

In this study we identify a new ground motion prediction equation applicable up to the moment magnitude (Mw) 9 using the strong motion records of the 2011 Tohoku-oki earthquake. First we determine base model with moment magnitude and shortest distance from the source fault as parameters. In order to avoid overestimations of amplitudes at magnitude larger than 8, we examine two models including a quadratic magnitude term or a completely amplitude saturation term at some Mw. And then we adopt additional correction terms corresponding to amplification by deep sediments and amplification by shallow soft soils, and anomalous seismic intensity distribution in order to improve predictions.

Keywords: Ground motion prediction equation, strong ground motion, the 2011 Tohoku-oki earthquake

1. INTRODUCTION

The ground motion prediction equation (GMPE) based on actually observed records is one of the useful tools in seismic hazard assessments. For instance, an equation for peak ground velocity (PGV) by Si and Midorikawa (1999) is used in assessing the national seismic hazard maps for Japan published by the Headquarters for Earthquake Research Promotion of Japan. The applicability of the existing GMPE for earthquakes of magnitude 9 has not been valid since the strong-motion records of such earthquakes had not been existed. The Tohoku-oki earthquake (moment magnitude Mw=9.0; hereafter Mw9) occurred on March 11, 2011 was the largest event that recorded by dense strong-motion observation networks in Japan. In this paper we first validate the applicability of the existing Japanese GMPEs for the earthquake of Mw9. And then we suggest a new GMPE directly applicable up to Mw9 based on the strong-motion records of the 2011 Tohoku-oki earthquake.

2. COMPARISON OF EXISTING GROUND MOTION EQUATIONS WITH OBSERVED RECORDS DURING THE 2011 TOHOKU-OKI EARTHQUAKE

Figure 1 shows a comparison between existing Japanese GMPEs with strong-motion records of the Tohoku-oki earthquake for peak ground acceleration (PGA) or velocity (PGV). We use observed records from National Research Institute for Earth Science and Disaster Prevention (NIED; K-NET and KiK-net; Aoi et al., 2011), Japan Meteorological Agency (JMA) and Port and Airport Research Institute (PARI). A band-pass filter from 0.1 to 10 Hz was applied to all records. The peak value is defined as the peak square root of the sum of squares of two orthogonal horizontal components in time domain through this study. Since all of the GMPEs used the shortest distance from source fault(s) as the source distance (X), we set the source fault to calculate the distance based on the evaluation by Earthquake Research Committee of Japan (2011) in Figure 1(c). In the figure we extrapolate Mw9 to all GMPEs. Note that distances larger than 300 km are also extrapolated. All GMPEs except for PGV from Si and Midorikawa (1999) can obtain peak amplitudes on an average ground condition in Japan. Since PGV on stiff soil site whose average S-wave velocity up to 30 m depth (Vs30) is 600 m/s can be

obtained from Si and Midorikawa (1999), we convert it by using the method of Matsuoka and Midorikawa (1993).

The existing GMPEs overestimate observations except for PGAs at near source region (<100 km). One possible reason of this overestimates is that all of the GMPEs in figure 1 modelled with a linear magnitude term. On the other hand, all the GMPEs include a magnitude-depend distance-saturation term. Therefore the predicted PGA at a short distance does not become large too much according to the saturation effect.

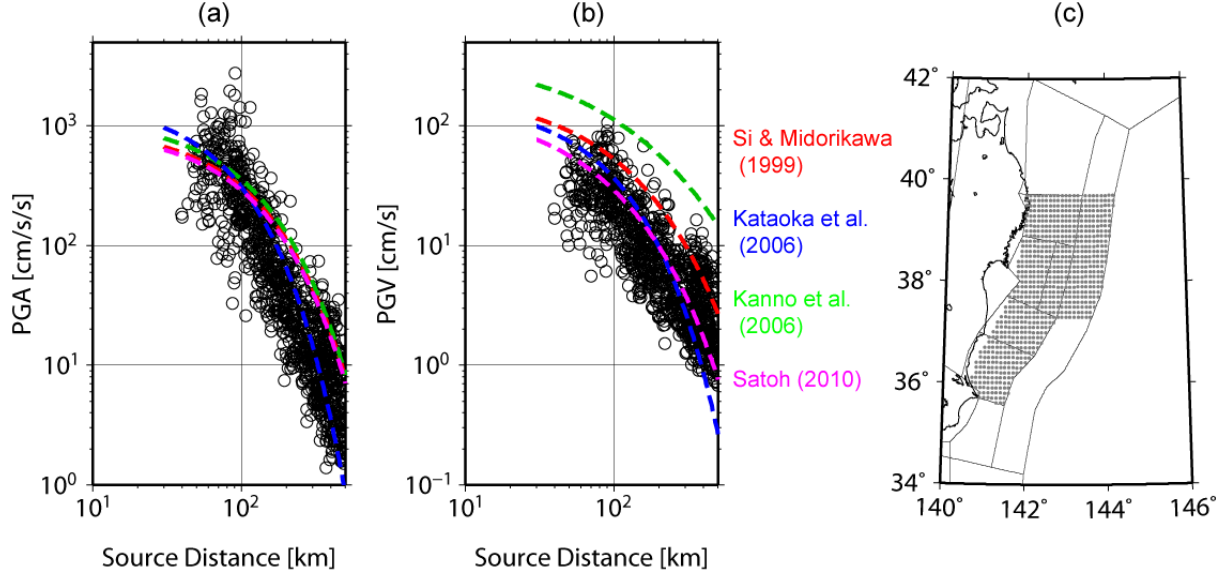


Figure 1. Comparison Between Existing GMPEs and Observed Records of the 2011 Tohoku-oki Earthquake

3. DATA

We update the strong-motion database of Kanno et al. (2006) by adding the strong-motion records up to the end of 2009. We collected waveform data from NIED, JMA and PARI. We use M_w determined by F-net, NIED. We also collected all available source fault models to calculate source distances. We also add the strong-motion records of the 2011 Tohoku-oki earthquake used in the previous section.

We selected data from the database for regression analysis using the following criteria: (1) M_w is not smaller than 5.5; (2) data were recorded on the ground surface; (3) two orthogonal horizontal components are available; (4) at least 5 stations were triggered by the event; (5) source distance is not larger than 200 km; and (6) data were truncated at source distance that predicted PGA by Kanno et al. (2006) was smaller than 10 cm/s/s.

4. BASE MODEL

First we obtain simple base model only M_w and shortest distance from source fault(s) (X ; hereafter source distance) as the parameters. Here we model subduction earthquakes and crustal earthquakes individually since the path effects are largely different between the two types. The target strong-motion parameters are the seismic intensity in JMA scale (I_j), PGA, PGV and the 5% damped acceleration spectra (SA). The period range of the acceleration spectra is from 0.05 to 10 seconds. The magnitude-distance distribution of strong-motion data used in this regression analysis are shown in Figure 2.

In order to examine modelling of a magnitude term, we first assume the following model

$$\log pre = \sum_{i=1}^N \alpha_i + bX - \log X, \quad (1)$$

where i is the suffix of the earthquake, N is the number of earthquakes. The relationship between Mw and the constant term α_i determined for each earthquake is shown in Figure 3. The saturation of α_i can be seen at Mw larger than about 8 from the figure. We examine two models to express such saturation. The model-1 is expressed with a quadratic magnitude term

$$\log pre = a_1 \cdot (Mw - Mw_{01})^2 + b_1 X + c_1 - \log(X + d_1 \cdot 10^{e_1 \cdot Mw}) \pm \sigma_1. \quad (2)$$

The other model (model-2) is expressed with a completely amplitude saturation at a Mw_{02}

$$\log pre = a_2 \cdot Mw' + b_2 X + c_2 - \log(X + d_2 \cdot 10^{e_2 \cdot Mw'}) \pm \sigma_2, \quad (3)$$

$$Mw' = \min(Mw, Mw_{02}). \quad (4)$$

Here a, b, c, d, e are regression coefficients and σ is the standard deviation. We use ten-base logarithm throughout this study. Note that "log pre" changes to "pre/2" in the case of Ij considering the definition of Ij. In this analysis we assumed that Mw_0 and e take a constant value independent of both earthquake type (subduction or crustal) and strong-motion parameter. After the trial-and-error approach, we fixed the values to $Mw_{01}=16.0$, $Mw_{02}=8.3$, $e_1=0.3$ and $e_2=0.5$, respectively. Then other coefficients are obtained by using the two-step stratified regression analysis method of Fukushima and Tanaka (1990). Finally obtained coefficients and base models are shown in Figure 4 and Figure 5, respectively. Figure 6 shows an example of the comparison between observed data and our new base models. Both models match to observations well in a wide magnitude range.

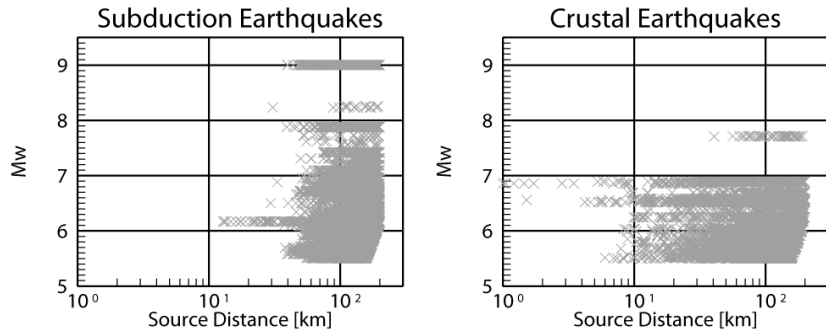


Figure 2. Magnitude-Distance Distribution of Used Data in Regression Analyses

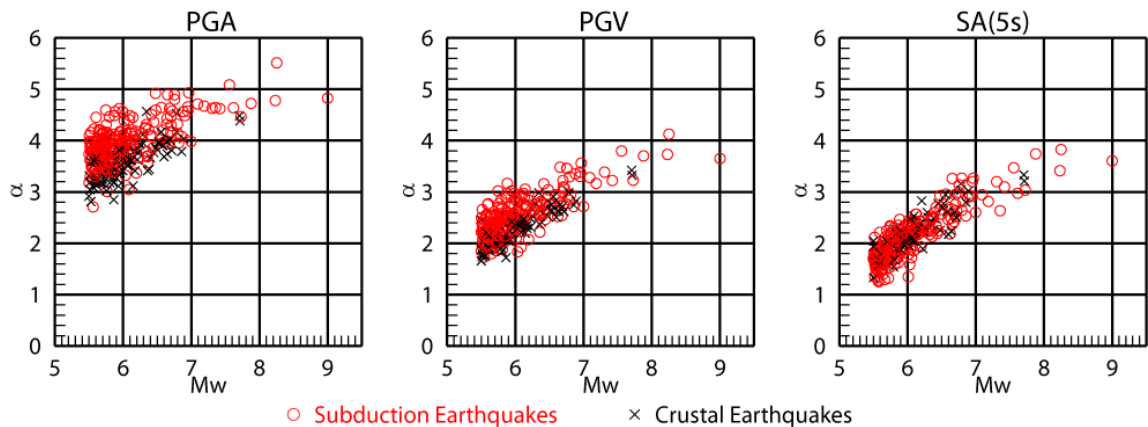


Figure 3. Example of Relation Between Coefficient α and Moment Magnitude

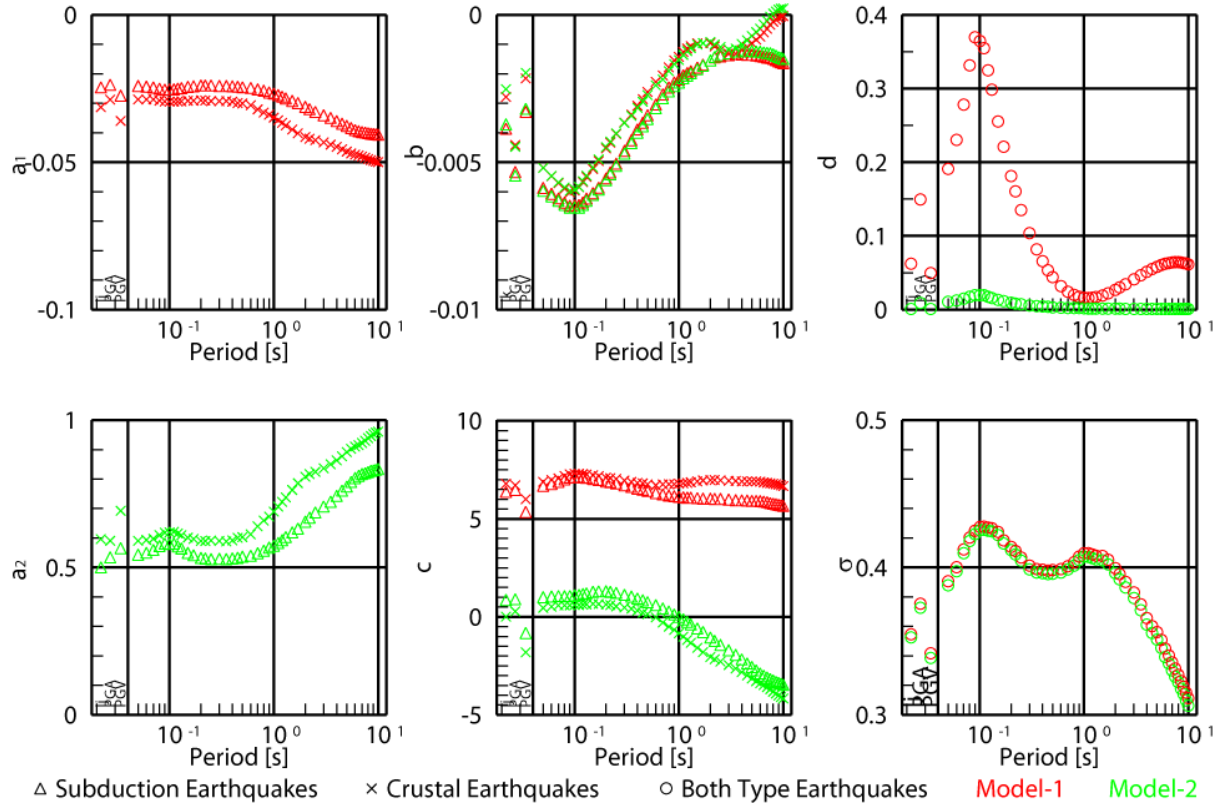


Figure 4. Obtained Coefficients for Equation (2) or (3)

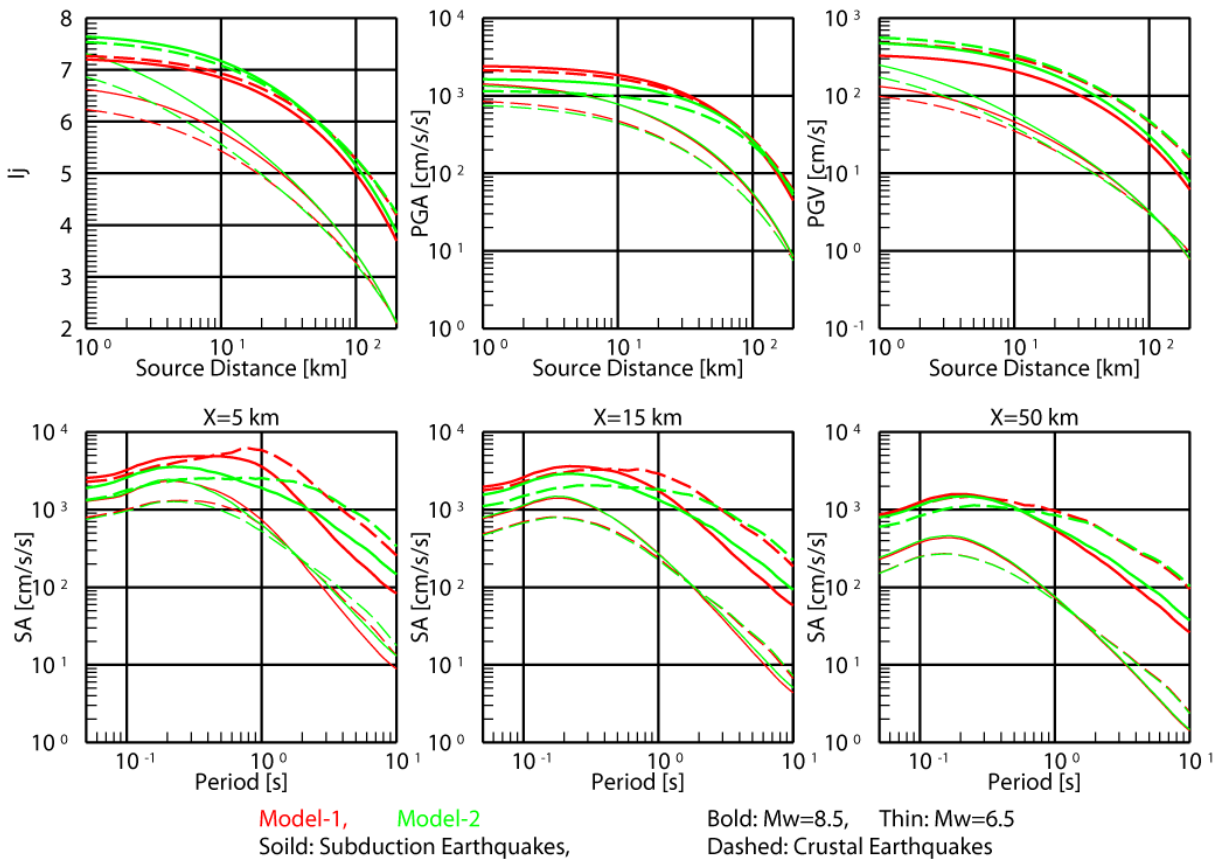


Figure 5. Example of Obtained Base Model of New GMPE

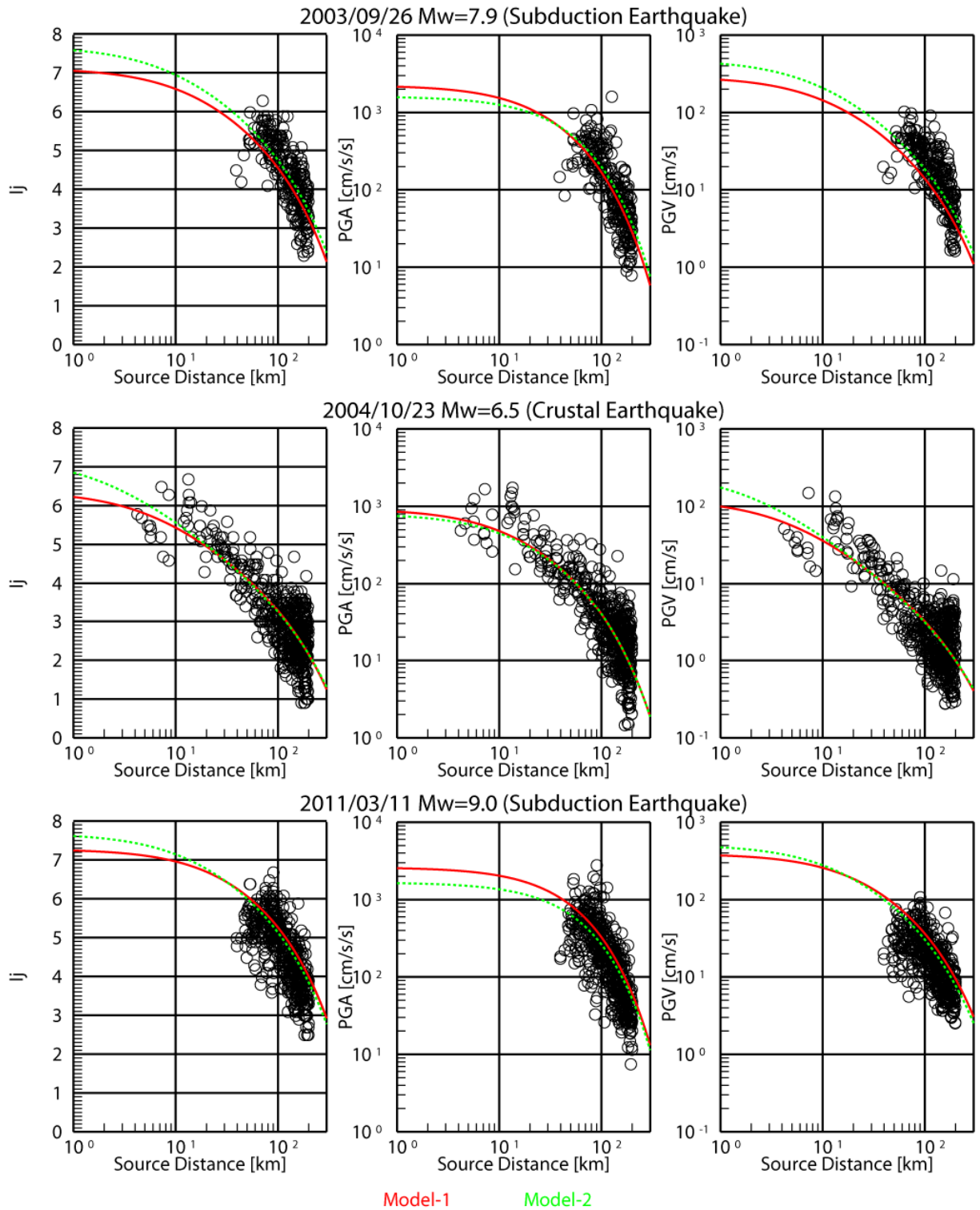


Figure 6. Example of Comparison Between Base Model and Observed Records

5. ADDITIONAL CORRECTION TERMS

Next we examine additional correction terms to improve accuracy of prediction results much more. Here we use the residual data between observed amplitude and predicted one calculated from the base model. Strictly speaking, the residual data from model-1 differ from the data from model-2, but we use

only the residual data from model-2 in this analysis.

5.1. Amplification by Deep Sedimentary Layers

To examine amplification characteristics by deep sedimentary layers, we extract data from whole data used in the above regression analysis using the following criteria: (a) Focal depth is shallower than 30 km; and (b) observed peak ground acceleration is smaller than 100 cm/s/s. The former is to avoid anomalous seismic intensity distribution mentioned in the section 5.3. The latter is to avoid non-linear site responses.

Fujiwara et al. (2009) constructed an underground structure model of deep sedimentary layers for whole Japan. Their model mainly consists of 6 layers whose S-wave velocity (V_s) is 600, 1100, 1400, 1700, 2100, 2700 m/s, respectively, on the seismic bedrock whose V_s is 3100 m/s or more. Because there are quite few sites on the basin area which seismic velocity profile to the seismic bedrock is available, we used this underground structure model in this study. Figure 7 shows an example that the relation between the residual and depth to each layer at the site. We can see the tendency that the residual becomes larger so that the top depth to the layer becomes deep. We model such tendency as below

$$G_{deep} (= \log[obs / pre]) = \begin{cases} q_d & D_l \leq D_{l0} \\ p_d \cdot \log(D_l / D_{l0}) + q_d & D_l > D_{l0} \end{cases} \quad (5)$$

where D_l is the top depth to the layer whose S-wave velocity is l (m/s) at the site, and p_d and q_d are the regression coefficients. We determine D_{l0} by the trial-and-error approach. Obtained coefficients are shown in Figure 8. The standard deviations before and after applying the correction are also shown in the figure. We find that this correction is needless for acceleration spectra at the period less than 0.3 seconds and PGA. The standard deviation takes a smallest value in the case of the top depth to the $V_s=1400$ m/s layer (D_{1400}) as a parameter for all periods including Ij, PGA and PGV. So we suggest the additional correction term corresponding to amplification by deep sedimentary layers with D_{1400} .

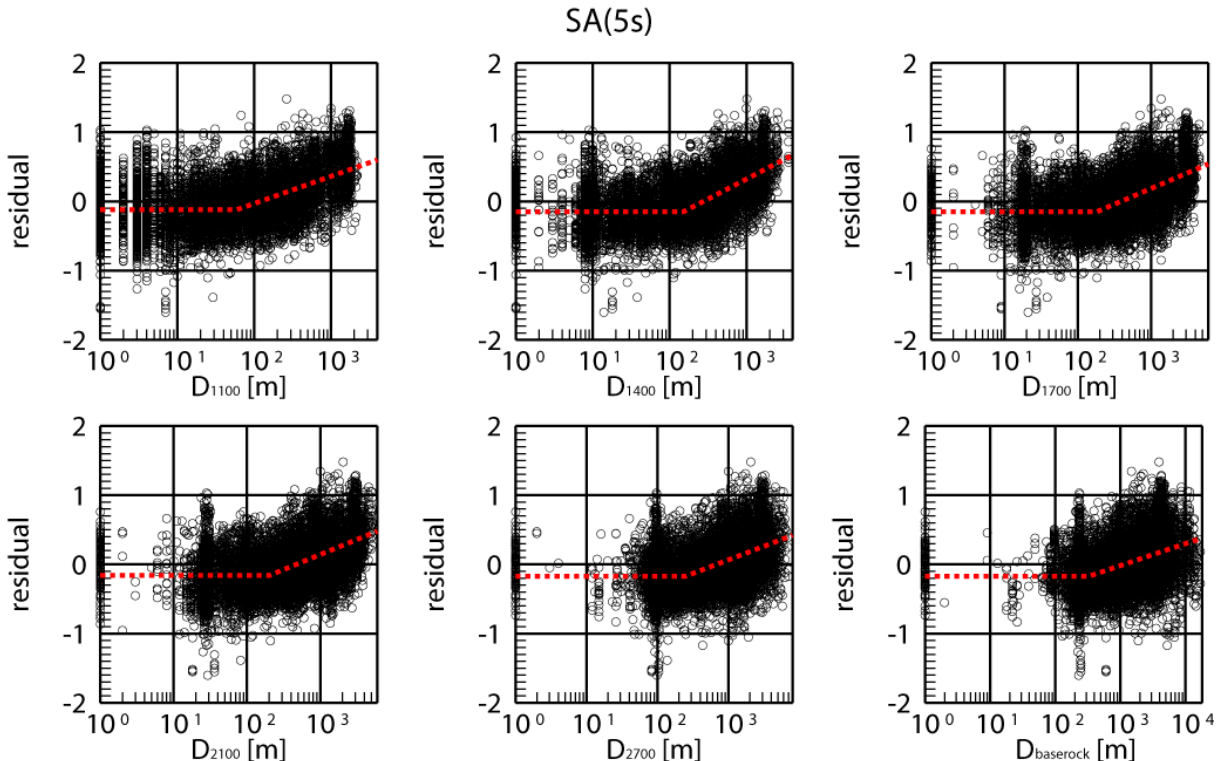


Figure 7. Example of Relation Between Residuals and D_l

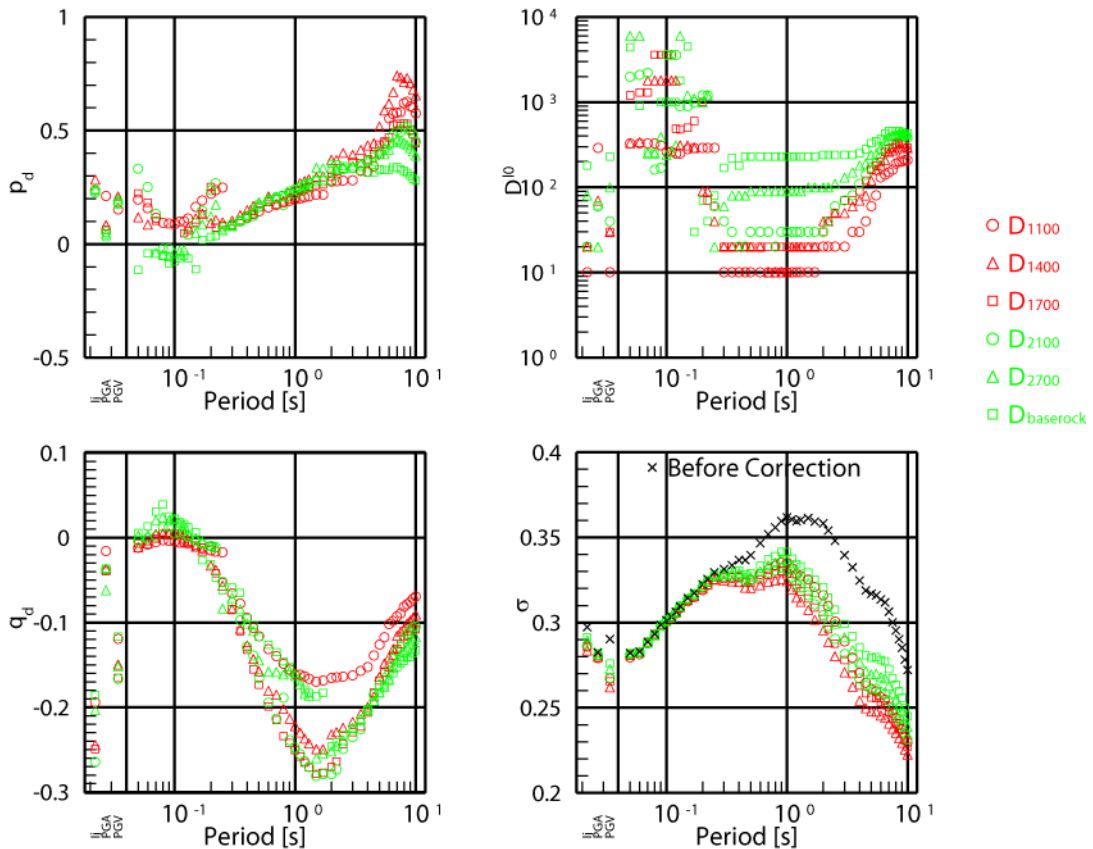


Figure 8. Obtained Coefficients for Deep Sediments Correction Term

5.2. Amplification by Shallow Soft Soils

The average S-wave velocity up to 30 m depth (V_{s30}) at an observation station is one of useful parameters to estimate amplification by shallow soft soils (e.g. Joyner and Fumal, 1984). Based on the 7.5-arc-second engineering geomorphologic classification map, Matsuoka and Wakamatsu (2008) constructed V_{s30} map which covered whole Japan. So we adopt the additional correction term corresponding to the amplification by shallow soft soils using V_{s30} as a parameter. The V_{s30} is defined as

$$V_{s30} = 30 / \sum_{l=1}^n (H_l / V_{s_l}), \quad (6)$$

where n is the number of strata layers down to depth 30 m, H_l and V_{s_l} denote the thickness (m) and S-wave velocity (m/s) of the l -th layer, respectively. To examine amplification characteristics by shallow soft soils, we extract data from whole data used in the above regression analysis using the following criteria: (a) Focal depth is shallower than 30 km; (b) observed peak ground acceleration is smaller than 100 cm/s 2 ; and (c) S-wave profile up to 20 m depth is known. In order to use many K-NET sites with PS-logging down to a depth of 20 m, we apply the relation between V_{s30} and V_{s20}

$$V_{s30} = 1.13V_{s20} + 19.5 \quad (7)$$

by Kanno et al. (2006). In order to avoid a double correction of site amplification, we adopt " pre_{Gd} " instead of " pre " in this section, which is the predicted amplitude calculated from the base model with the correction by equation (5). Figure 9 shows an example of the relation between the residual and V_{s30} . We can see the tendency that the residual becomes smaller so that the V_{s30} becomes larger. We model such tendency as below

$$G_{shallow} (= \log[obs / pre_{Gd}]) = \begin{cases} p_s \cdot \log Vs30 + q_s & Vs30 \leq Vs30_0 \\ p_s \cdot \log Vs30_0 + q_s & Vs30 > Vs30_0 \end{cases}, \quad (8)$$

where p_s and q_s are the regression coefficients. We determine $Vs30_0$ by the trial-and-error approach. Obtained coefficients are shown in Figure 10. The standard deviations before and after applying the correction are also shown in the figure. The correction is the most effective to the period around 1 second. As shown in Figure 10, the zero-crossing point is stably obtained approximately 350 m/s in almost all period range. This value is slightly larger than approximately 300 m/s by Kanno et al. (2006).

This type correction, however, cannot express the difference in the predominant period among variety of site conditions. Therefore, this correction should be applied to obtain the amplitude on an engineering bedrock rather than that on the ground surface.

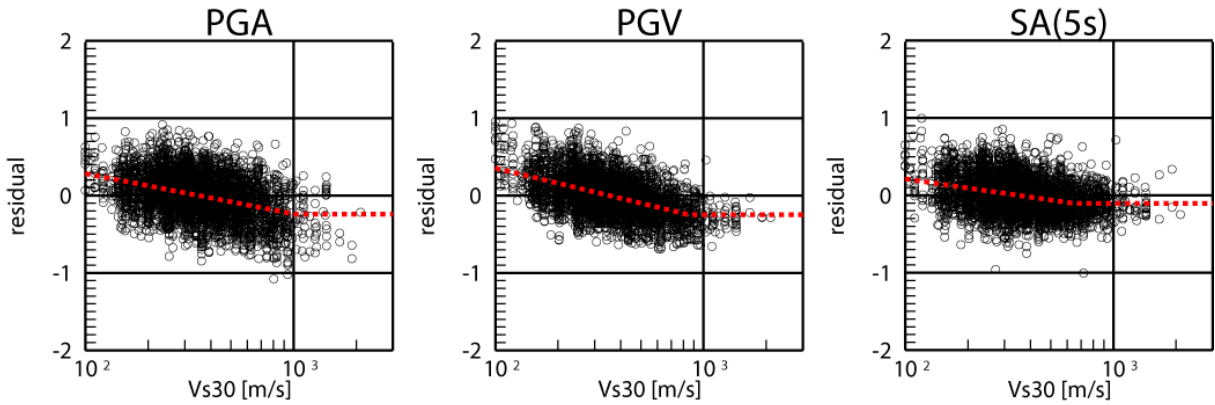


Figure 9. Example of Relation Between Residual and Vs30

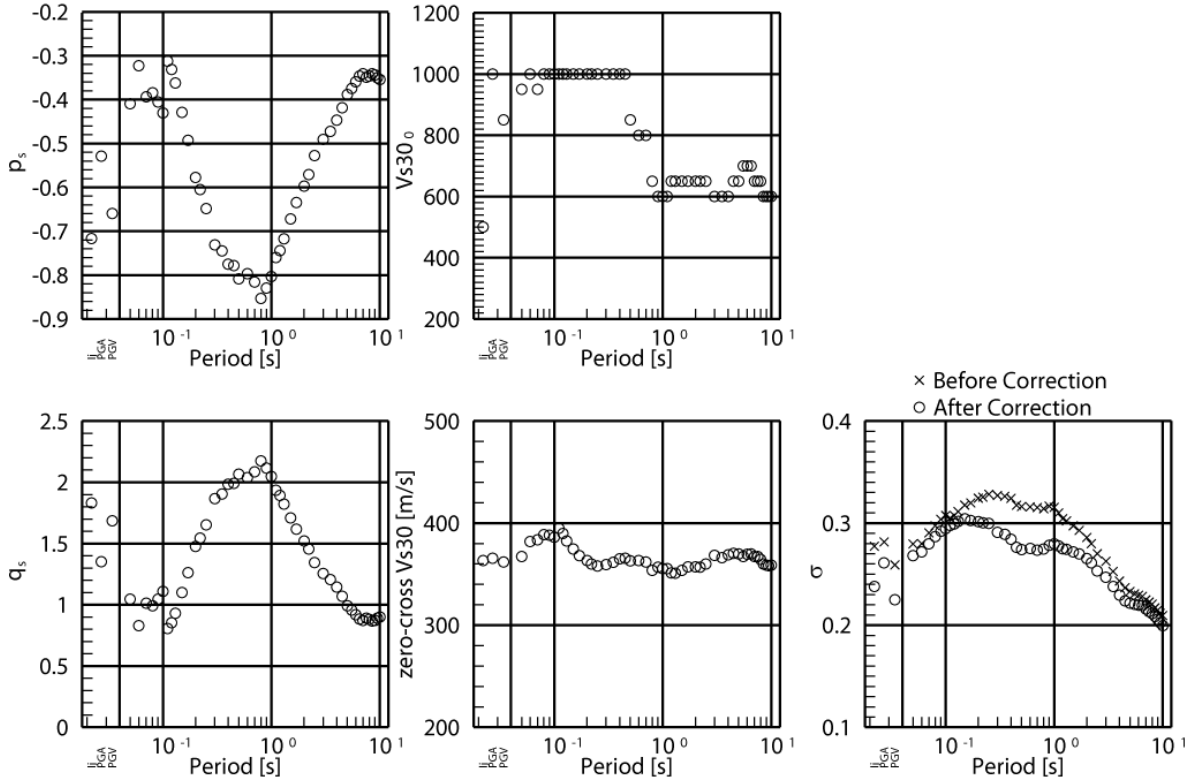


Figure 10. Obtained Coefficients for Shallow Soft Soils Correction Term

5.3. Anomalous Seismic Intensity Distribution

Anomalous seismic intensity distribution can be seen during the intermediate-depth and deep earthquakes. This phenomenon is explained by a unique attenuation (Q) structure beneath the island-arc region as shown in Figure 11(a). In order to express such phenomenon, Morikawa et al. (2006) suggest additional correction terms using the distance from volcanic front to observation site (X_{vf} in Figure 11(a)) as the parameter. The model is expressed as below

$$AI = \log[obs / pre_G] = \gamma \times X_{vf} \times (H - 30), \quad (9)$$

where H is the focal depth of the earthquake (km) and γ is the regression coefficient. In this section we adopt " pre_G " instead of " pre " or " pre_{Gd} ", which is the predicted amplitude calculated from the base model with the corrections by equations (5) and (8). Note that only earthquakes deeper than 30 km should be applied this correction. To examine anomalous seismic intensity distribution, we extract data from whole data used in the above regression analysis using the following criteria: (a) Focal depth is deeper than 30 km; and (b) observed peak ground acceleration is smaller than 100 cm/s/s. The coefficient should be obtained for northeast Japan (earthquakes occurring at the Pacific Plate) and southwest Japan (earthquakes occurring at the Philippine Sea Plate) individually. The results are shown in Figure 11(b). The standard deviations before and after applying the correction are shown in the figure 11(c), but we use data of earthquakes deeper than 60 km there because the anomalous seismic intensity distribution is not so clear in shallower earthquakes. We find that the correction is quite valuable for short period range including Ij, PGA and PGV while it is needless for periods longer than 2 seconds. The γ values for northeast Japan are about half of those in Morikawa et al. (2006), and smaller than those for southwest Japan at period range. This may be caused by a complexity of a Q-structure beneath northeast Japan.

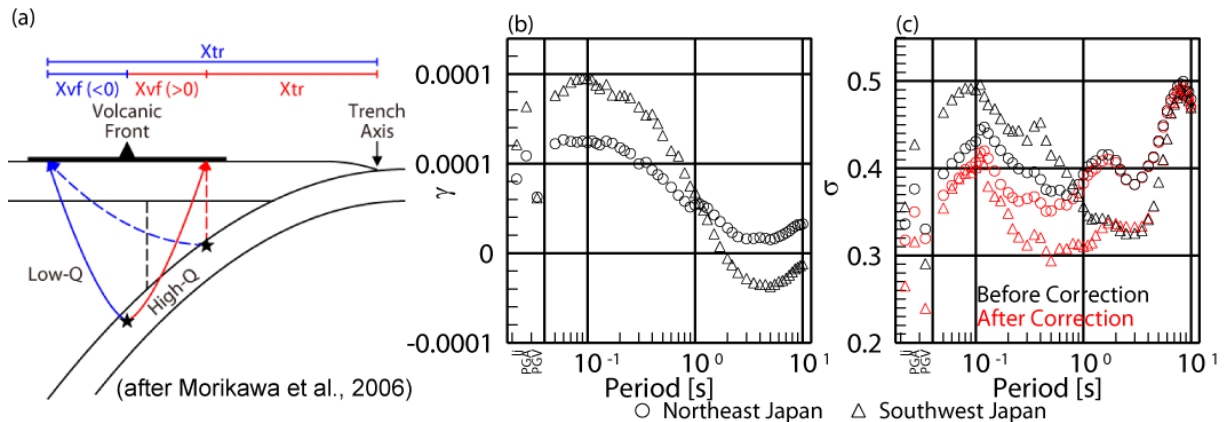


Figure 11. Obtained Coefficients for Anomalous Seismic Intensity Distribution Correction Term

6. CONCLUSIONS

In this study we identify a new ground motion prediction equation applicable up to Mw9 by using strong motion data of the 2011 Tohoku-oki earthquake. Our target is not only peak amplitudes but also response spectra. We examine two kinds of base models to express the amplitude saturation at large magnitudes but we cannot decide which model is better yet. We also adopt three additional correction terms that should be applied to base models to improve predictions. A much number of large aftershocks of the 2011 Tohoku-oki earthquake, however, have occurred after the main shock. We should have regression analyses again after adding these strong-motion records to our database.

ACKNOWLEDGEMENT

Strong-motion records used in this study were provided from NIED, JMA, PARI, Central Research Institute of Electric Power Industry, Hanshin Expressway Public Corporation, Honshu-Shikoku Bridge Authority, Japan Railway Company Group, Kansai Electric Power Company, Kobe City Office, Konoike Construction, Co., Ltd., Kyoto University, Maeda Corporation, Matsumura-gumi Corporation, National Institute for Land and Infrastructure Management, Nippon Telegraph and Telephone Corporation, Obayashi Corporation, Osaka Gas Co., Ltd., Railway Technical Research Institute, Shiga Prefecture, The Committee of Earthquake Observation and Research in Kansai Area, The University of Shiga Prefecture, and Tokyo Electric Power Company. We thank all of these organizations. This study was conducted as a part of the research on advanced seismic hazard assessment for the national seismic hazard maps for Japan.

REFERENCES

- Aoi, S., Kunugi, T., Nakamura, H. and Fujiwara, H. (2011). Deployment of New Strong Motion Seismographs of K-NET and KiK-net, in *Earthquake Data in Engineering Seismology, Geotechnical, Geological, and Earthquake Engineering*, Springer, **14**, 167-186.
- Earthquake Research Committee of Japan (2011). The 2011 off the Pacific Coast of Tohoku Earthquake (April 11), <http://www.jishin.go.jp/main/index-e.html>.
- Fukushima, Y. and Tanaka, T. (1990). A new attenuation relation for peak horizontal acceleration of strong motion in Japan, *Bulletin of the Seismological Society of America*. **86**, 329-336.
- Joyner, W. B. and Fumal, T. E. (1984). Use of measured shear-wave velocity for predicting geologic site effects on strong ground motion. *Proceedings of 8th World Conference on Earthquake Engineering*. **2**, 777-783.
- Kanno, T., Narita, A., Morikawa, N., Fujiwara, H. and Fukushima, Y. (2006). A new attenuation relation for strong ground motion in Japan based on recorded data, *Bulletin of Seismological Society of America*. **96**, 879-897.
- Kataoka, S., Satoh, T., Matsumoto, S. and Kusakabe, T. (2006). Attenuation relationships of ground motion intensity using short period level as a variable. *Journal of Japan Society of Civil Engineers A*. **62**, 740-757 (in Japanese with English abstract).
- Matsuoka, M. and Midorikawa, S. (1983). Empirical estimateion of average shear-wave velocity of ground using the Digital National Land Information, *Journal of Structural and Construction Engineering (Transactions of AIJ)*. **443**, 65-71 (in Japanese with English abstract).
- Matsuoka, M. and Wakamatsu K. (2008). Site amplification capability map based on the 7.5-arc-second Japan engineering geomorphologic classification map. *National Institute of Advanced Industrial Science and Technology, Intellectual property management*. No. H20PRO-936.
- Morikawa, N., Kanno, T., Narita, A., Fujiwara, H. and Fukushima, Y. (2006). Additional Correction Terms for Attenuation Relations of Peak Amplitdes and Response Spectra Corresponding to the Anomalous Seismic Intensity in Northeastern Japan, *Journal of Japan Earthquake Engineering Society*. **6:1**, 23-41 (in Japanese with English abstract).
- Satoh, T. (2010). Attenuation relations of horizontal and vertical ground motions for intraslab and interplate earthquakes in Japan. *Journal of Structural and Construction Engineering (Transactions of AIJ)*. **647**, 67-76 (in Japanese with English abstract).
- Si, H. and Midoriakwa, S. (1999). New attenuation relationships for peak ground acceleration and velocigy considering effects of fault type and site condition, *Journal of Structural and Construction Engineering (Transactions of AIJ)*. **523**, 63-70 (in Japanese with English abstract).